J Therm Anal Calorim (2017) 130:123–130
DOI 10.1007/s10973-017-6232-5

Al_2O_3/Ni functionally graded materials (FGM) obtained by centrifugal-slip casting method

Justyna Zygmuntowicz[1] · Paulina Wiecińska[2] · Aleksandra Miazga[1] · Katarzyna Konopka[1] · Waldemar Kaszuwara[1]

Received: 26 October 2016 / Accepted: 21 February 2017 / Published online: 4 March 2017

Abstract The fabrication and the characterization of Al_2O_3/Ni composites with a gradient distribution of the Ni particles are reported. The composites have been obtained by centrifugal-slip casting and subsequent sintering and had the shape of a hollow cylinder. TG/DTA analysis was done for the nickel powder with the addition of the dispersant used in centrifugal-slip casting as well as for the composite green body. The measurements were performed in two atmospheres: argon and the mixture of argon and hydrogen (1:1). Additionally, coupling the thermobalance with the mass spectrometer allowed to determine type of gases released from the samples during thermal treatment. The morphology and chemical composition of the produced composites were analyzed using a scanning electron microscope equipped with an EDS detector. Interface between alumina and nickel was described. Moreover, the X-ray diffraction was made. The stereological analysis confirmed that the nickel particles are distributed in the composite in a gradient way.

Keywords Centrifugal-slip casting · Al_2O_3/Ni · Composite · Reductive atmosphere · TG/DTA · Mass spectrometry

✉ Justyna Zygmuntowicz
justyna.zygmuntowicz@inmat.pw.edu.pl

[1] Faculty of Materials Science and Engineering, Warsaw University of Technology, 141 Woloska St, 02-507 Warsaw, Poland

[2] Faculty of Chemistry, Warsaw University of Technology, 3 Noakowskiego St, 00-664 Warsaw, Poland

Introduction

Functionally graded materials (FGM) are a novel group of materials characterized by continuous spatial distribution of two or more components. Because of special properties of materials from this group, they are becoming more widely studied [1–4]. In particular, ceramic–metal FGM composites, for example Al_2O_3/Ni, have advantageous properties such as effective thermal stress relaxation, high hardness, high fracture toughness and good corrosion resistance. They can be used in many applications ranging from aerospace to chemical industry [5, 6]. Several methods have been proposed to obtain gradient distribution of metallic particles in a ceramic matrix, for example slip casting with magnetic field or the powder metallurgical process applied for: Al_2O_3/Fe, SiC-AlN/Mo [7, 8]. Authors have obtained FGM samples by centrifugal-slip casting which is an innovative, relatively simple and effective shaping method [9]. A combination of classical slip casting with centrifugal force for alumina/nickel system allows to receive variable distribution of the metallic particles in a composite material. The gradient is obtained due to the different speeds in liquid medium of particles with different density [10]. The technology of the preparation of composites with a zonal distribution of the metallic phase by centrifugal-slip casting can be used for producing composite sleeve-shaped parts with a metallic phase concentration gradient (intended, e.g., for transporting a toxic medium) or parts with increased mechanical strength. The prepared suspensions for centrifugal-slip casting process contain the mixture of ceramic and metallic powders, solvent and deflocculants. It is important that used additives are non-toxic and harmless to the environment during the sintering process. For this reason, as a solvent in most cases the distilled water is used [11]. In aqueous media, nickel

powder can undergo hydroxylation and the thin nickel oxide layer present on its surface can be converted to $Ni(OH)_2$ or NiO(OH) [12]. In the case of the application of metallic powder with micrometric size, the amount of formed compounds is minimal and should be reduced during the sintering process. It is worth to underline that the resulting sintered bodies have a high relative density and additionally strong connection between the components of the composite is observed. The quality of the fabricated elements strongly depends on sintering process. In the case of alumina-nickel composites, it is preferable to use a reductive atmosphere in order to prevent oxidation of the nickel surface, remove the compounds formed on the nickel particles surface and prevent its reaction with alumina leading to the formation of nickel aluminate spinel [13]. Moreover, it is significant that organic additives are completely burned out and will not affect the microstructure of the fabricated composite materials. In the literature, there are several researches on the sintering of ceramic-based materials in air or protective gases such as argon [14]. There is little research on the analysis of the sintering process conducted in reducing atmosphere. For this reason, DTA/TG analysis gives important information about thermal degradation of additives used in shaping process as well as about the thermal behavior of samples in the inert and reductive atmospheres [15–18]. Furthermore, coupling mass spectrometer with thermobalance allows to detect type of gases released from samples. These studies allow to effectively plan the sintering process of the material.

Experimental

Alumina powder (Taimicron TM-DAR, Taimei Chemicals Co., Japan) with a mean particles size of 133 ± 30 nm and density 3.96 g cm^{-3}, and nickel powder (Sigma-Aldrich, Poland) with a mean particles size of 3 μm and density 8.9 g cm^{-3} were used for the preparation of the suspensions. The purity of both powders was 99.99%. Diammonium hydrocitrate (DAC, puriss, POCh, Poland) and citric acid (CA, ≥99.5% Sigma-Aldrich, Poland) were used as dispersants in the ceramic slurries in an amount 0.3 and 0.1 mass% with respect to powders content, respectively. The selection of dispersant was made based on previous research [11, 19].

The aqueous ceramic slurries containing 50 vol% of the solid phase and including 10 vol% of the nickel particles were made. The slurries were prepared by adding the alumina and nickel powders to the water with deflocculants and milling the mixture in a planetary ball mill with rotational speed of 300 rpm for 60 min. The aqueous suspensions were poured into a gypsum mold with the inner diameter of 20 mm. Then, the tubular mold was centrifuged in the radial direction with speed of 1000 rpm for 3 h. After the centrifugation, the sample together with the gypsum mold was removed from the metal mold and was dried in the vertical position in a dryer at 25 °C for 24 h. The dimensions of the gypsum mold were: the outer radius −40 mm, the thickness −10 mm, the length −60 mm and the inner radius −20 mm. The dried sample can be easily removed from the gypsum mold, thanks to the drying shrinkage. Then, the sample was sintered at 1400 °C in H_2/Ar atmosphere (Ar of 80 vol% and balance H_2). During the sintering, the heating and cooling rate were 5 °C min^{-1}. This process allowed to obtain composites in the shape of a hollow cylinder with gradient concentration of the nickel particles. Drying shrinkage in the case of centrifugal-slip casting is very low, negligible and therefore has not been determined. The sintering linear shrinkage equaled 12.84%.

The thermal analysis has been done for the nickel powder with the addition of the dispersants DAC and CA used in the preparation of Al_2O_3/Ni composites as well as for the obtained Al_2O_3/Ni green body. The purpose of the addition of the dispersants was to create the conditions similar to those in the suspensions used to prepare composite samples by centrifugal-slip casting. DTA/TG measurements were carried out by using Netzsch STA 449C coupled with Quadrupole Mass Spectrometer Netzsch QMS 403C. The heating rate was 10 °C min^{-1}, and the final temperature was 550 °C. The measurements were performed in two atmospheres: argon and the mixture of argon and hydrogen (1:1), and the total gas flow was 100 mL min^{-1}. The construction of the apparatus did not allow to perform the measurements with the high concentration of the hydrogen to higher temperatures due to the possible corrosion of platinum thermocouples. Mass spectrometer was set to detect m/z values in the range of 10–300. The research could show the possible presence of the oxidized form on the surface of nickel powder and the influence of the metal on the thermal characteristic of the Al_2O_3/Ni green body.

Samples for microstructure analysis were cut using a diamond wheel by precision cut-off machine Secotom 15 (Struers). The observed surface was prepared by using standard metallographic methods (grinding and polishing with diamond paste up to 1 μm). The microstructure of the cross section of sintered samples was examined by the scanning electron microscopes Hitachi S-3500N and SU-70. The elemental distribution of nickel, aluminum and oxygen in the cross section of the samples was analyzed by energy-dispersive X-ray spectroscopy (EDS). The EDS scan was taken at 15 kV.

The interface between alumina and nickel was observed on SEM/STEM HITACHI S 5500.

The analysis of the phase composition of obtained materials was performed using X-ray diffractometer

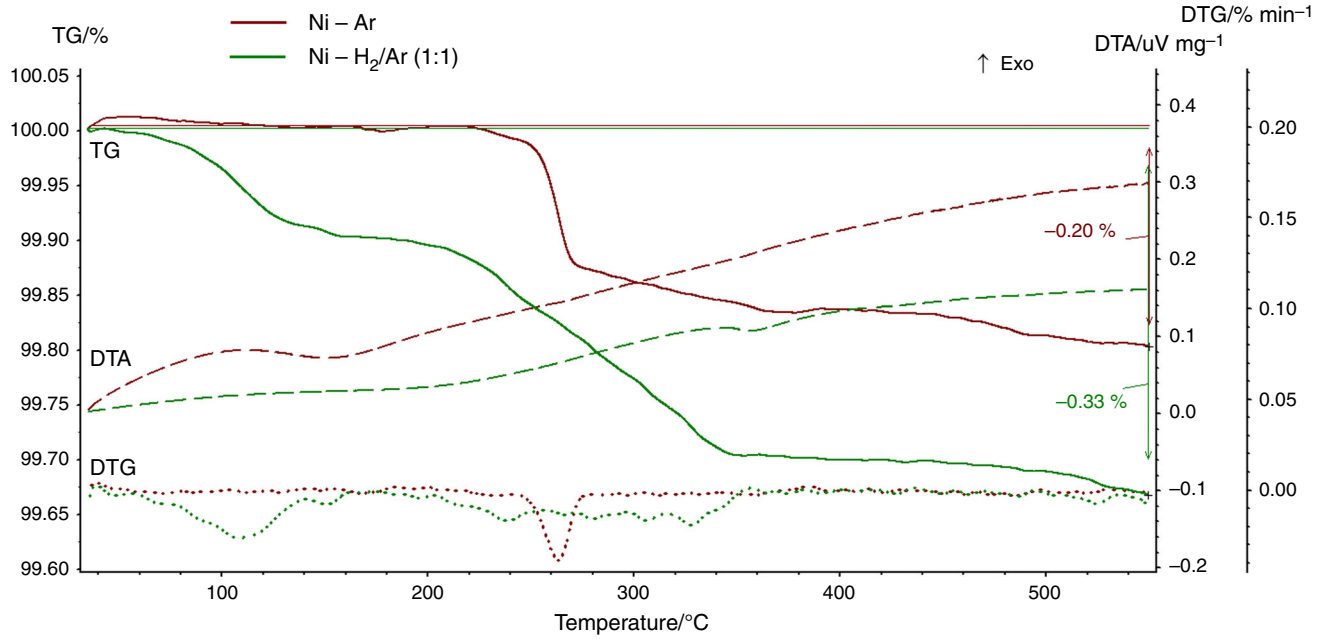

Fig. 1 DTA/TG/DTG curves registered in two atmospheres: argon and the mixture of hydrogen and argon (1:1) of nickel powder with the addition of the dispersants

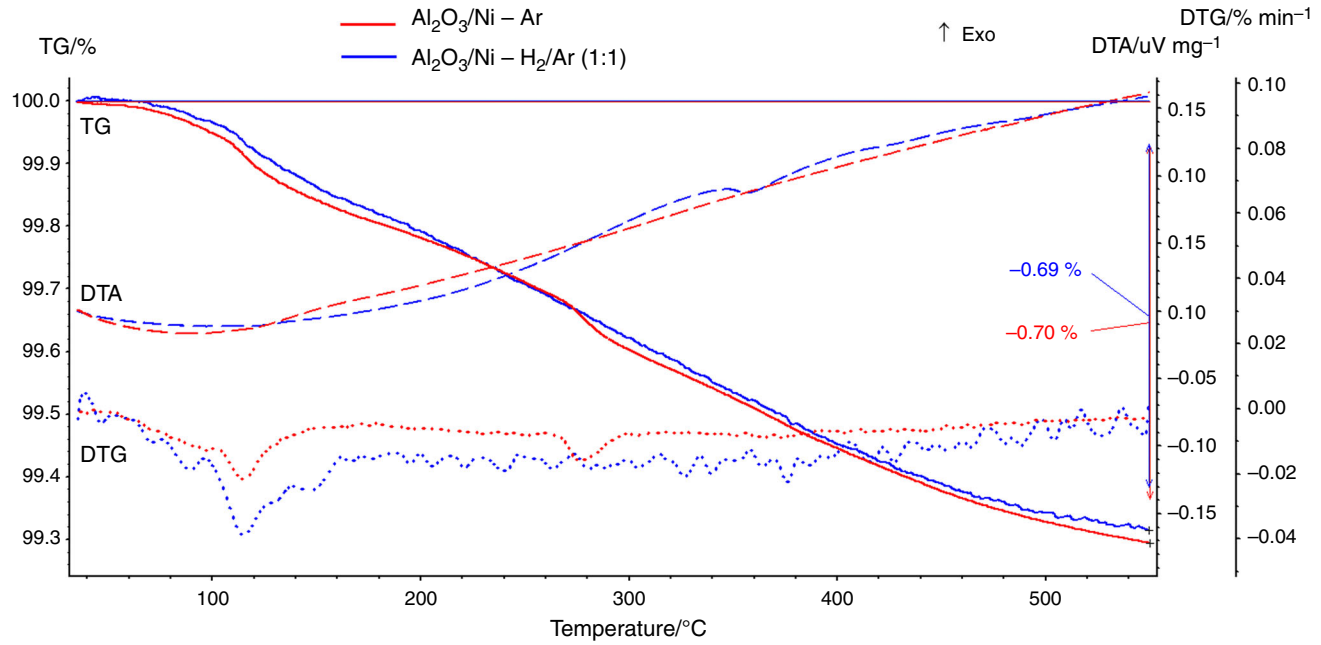

Fig. 2 DTA/TG/DTG curves registered in two atmospheres: argon and the mixture of hydrogen and argon (1:1) of Al_2O_3/Ni green body obtained by centrifugal-slip casting

Rigaku MiniFlex II. $CuK_{\alpha 1.54}$ was used with the value of the angle 10°–80° and a step size of 1°. The analyses were performed at the cross section of samples. For the identification of the component phases, crystallographic database ICCDD-PDF4-2014 has been used. The XRD patterns were recorded for two samples for reproducible results. The XRD study was performed on the radius of sintered sample.

The physical properties and the density of sintered bodies were determined by the Archimedes method according to the PN-76/E-06307. The relative densities of composite bodies were calculated using the rule of mixture.

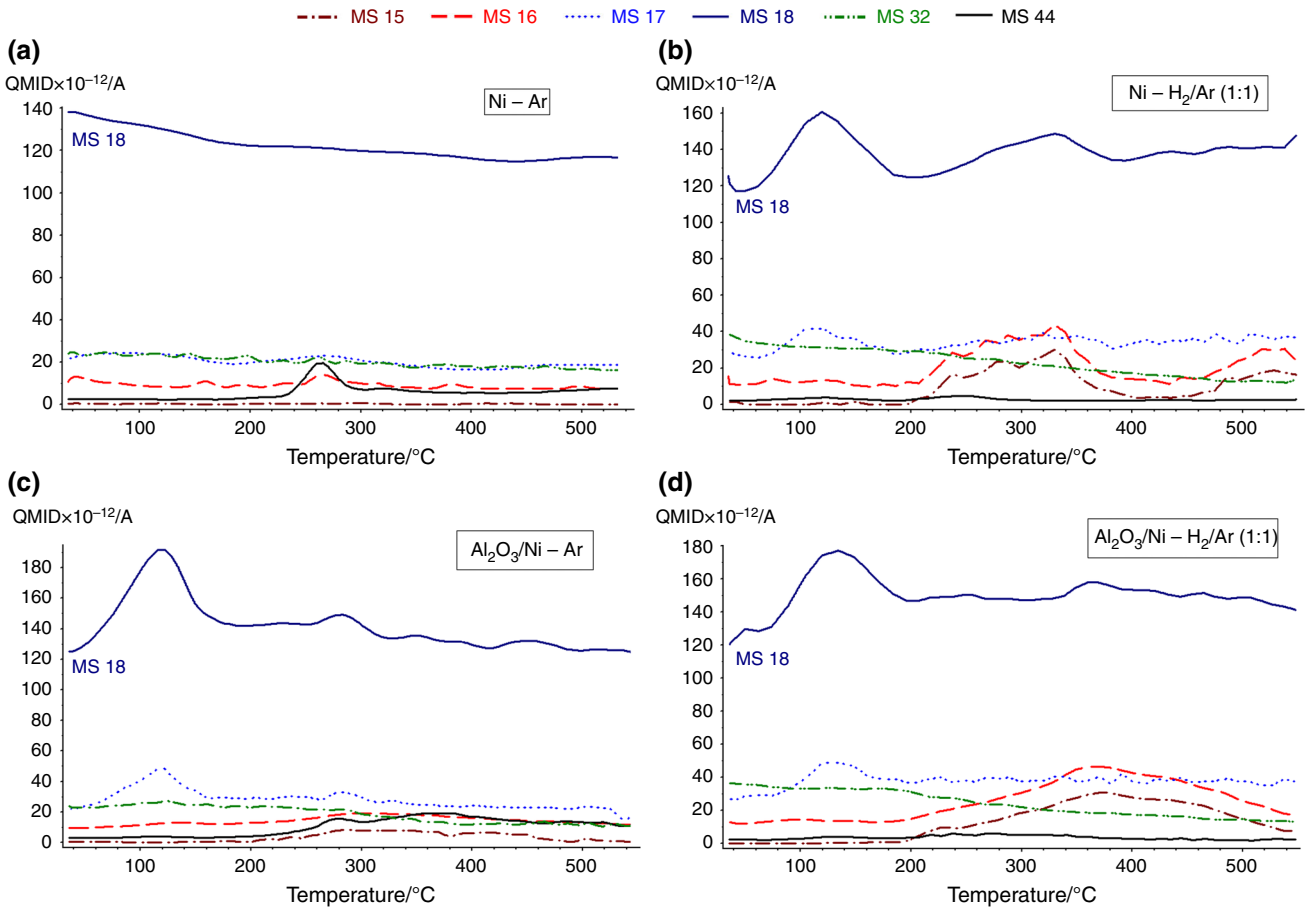

Fig. 3 m/z values registered by QMS as a function of temperature of samples measured in two atmospheres: Ni in Ar (**a**), Al_2O_3/Ni in Ar (**b**), Ni in H_2/Ar (**c**) and Al_2O_3/Ni in H_2/Ar (**d**)

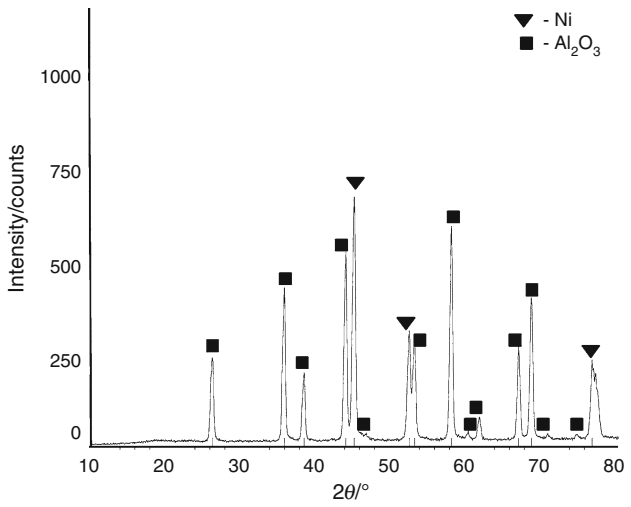

Fig. 4 X-ray diffraction pattern of the Al_2O_3/Ni composite

The values 3.96 and 8.9 g cm^{-3} as the theoretical densities of alumina and nickel, respectively, were used.

Quantitative description of the microstructure was made on the basis of SEM images of randomly selected areas on the samples using computer image analysis applying the program Micrometer [20]. This method allows obtaining information about the actual size and distribution of metallic phases in the sample. SEM analysis of images included: image processing, measurements and interpretation of obtained results. Microstructure observations were performed using magnification 1000×. The average values were calculated from measurement of 50 images. The nickel particles were described by parameter d_2—diameter of circle of the same surface as the surface of the analyzed grain [μm]. Based on the results of stereological analysis, average values of shape factors characterizing metal

Table 1 Selected properties of the Al_2O_3/Ni composite material

Property	Al_2O_3/Ni
Theoretical density/g cm^{-3}	4.45
Bulk density/g cm^{-3}	4.42 ± 0.02
Relative density/%	99.33 ± 0.40
Linear shrinkage (samples diameter)/%	12.84 ± 0.70

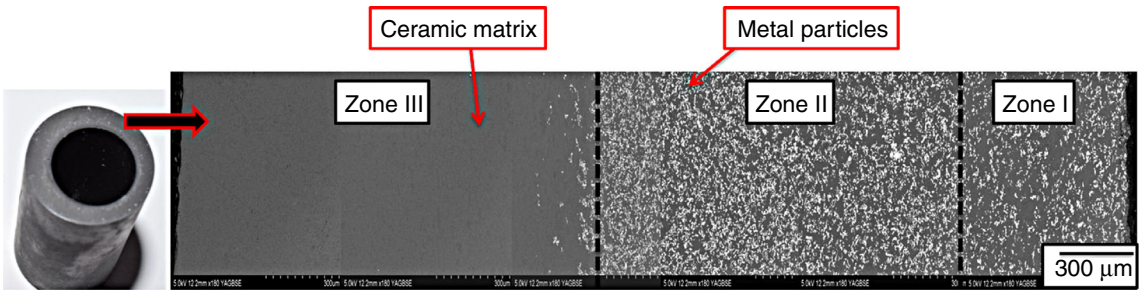

Fig. 5 SEM-BSE micrographs of the Al_2O_3/Ni composite

particles have been determined: elongation ($\alpha = d_{max}/d_2$), surface development ($R = p/(\pi \cdot d_2)$) and convexity ($W = p/p_C$), where d_{max}—maximum diameter of particle projection [µm], p—perimeter of particle [µm], p_C—Cauchy perimeter [µm] [20].

Results and discussion

Figure 1 presents DTA/TG/DTG curves of nickel powder with the addition of the dispersants DAC and CA. The total mass loss in the case of the sample measured in H_2/Ar (1:1) atmosphere was 0.33%, while for sample measured only in Ar—0.20%. The mass loss can be ascribed to the decomposition of the dispersants from the powder surface. On the other hand, the higher mass loss in the case of the second sample may indicate on the presence of the oxidized form on the surface of the nickel powder which has been reduced in hydrogen. Additionally, the changes on the TG curve in the case of the sample measured in H_2/Ar are observed since the beginning of the measurement, while for the sample measured in Ar, no changes on TG are visible till ca. 250 °C. More information can be gained from the results from the mass spectrometer coupled with the thermobalance, shown in Fig. 3 and discussed later in the text.

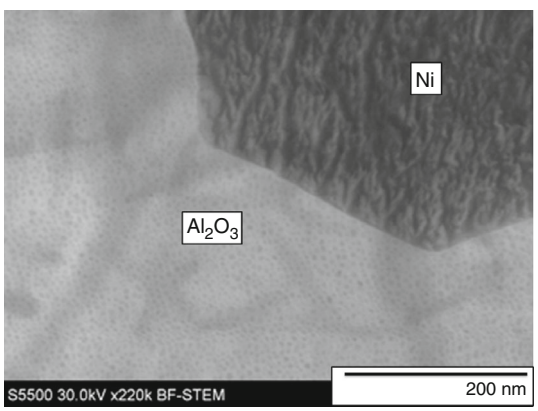

Fig. 6 The areas selected to EDS measurements

Figure 2 presents DTA/TG/DTG curves of Al_2O_3/Ni green body in which the concentration of the nickel was 10 vol%. Samples have been obtained by centrifugal-slip casting. The total mass loss was ca. 0.70% both for the sample measured in Ar and H_2/Ar (1:1). It indicates that in the case of the composite material no significant influence of the nickel on the thermal behavior of the material is observed. The mass loss indicates on the thermal decomposition of the organic additives and sample dehydration.

Mass spectrometer has detected six m/z values: 15, 16, 17, 18, 32 and 44. Masses 17 and 18 can be ascribed to H_2O, and mass 44 corresponds to CO_2. The presence of O_2 released from the samples could be confirmed by the increase of the intensities of masses 32 and 16, on the other hand, masses 15 and 16 having similar intensity can indicate on the presence of CH_4. Analyzing the data obtained for nickel measured in argon (Fig. 3a), it can be concluded that the only gaseous product which is released from the sample is CO_2 which comes from the decomposition of the dispersants. The situation is different in the case of the measurement carried out in the reductive atmosphere that is H_2/Ar (1:1). The increase of the intensities of masses 15 and 16 may indicate on methane which comes from the decomposition of organic dispersants, while the increase of the intensities of masses 17 and 18 can be ascribed to the dehydration of the sample. There is also the possibility that the nickel oxide which can be located on the nickel surface has been reduced to some substances, but due to the reaction with other gases the final compounds present in the gaseous mixture are H_2O, CH_4 and CO_2 (Fig. 3b). The similar conclusions can be drawn for the Al_2O_3/Ni samples, except that the increase of the masses 17 and 18 is observed for the measurements carried out both in argon and the mixture of hydrogen and argon. This can be explained by the higher amount of water present in the green bodies as a result of the shaping process (Fig. 3c, d). The most important similarity comparing the samples measured in Ar and H_2/Ar is that in the case of the measurements carried out in the inert atmosphere predominant gaseous product is CO_2, while in the reductive atmosphere it is probably CH_4. Oxygen is not observed as the gas reaching QMS detector.

Table 2 Mass and atomic content of selected elements from different areas

	Mass/%			Atomic/%			Volume/%
	O	Al	Ni	O	Al	Ni	Ni
Area 1	26.44 ± 0.92	54.87 ± 0.70	18.69 ± 2.64	41.27 ± 1.23	50.79 ± 0.65	7.95 ± 1.12	9.5 ± 1.33
Area 2	19.80 ± 0.69	44.10 ± 0.64	36.10 ± 2.91	35.49 ± 1.24	46.87 ± 0.68	17.63 ± 1.42	20.0 ± 1.60
Area 3	34.23 ± 0.80	62.65 ± 0.80	3.12 ± 0.97	47.39 ± 1.28	51.43 ± 0.65	1.18 ± 0.36	1.5 ± 0.46

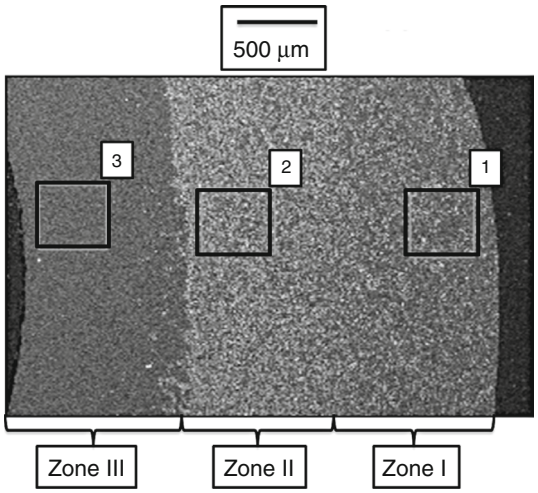

Fig. 7 STEM image of the interface between alumina and nickel in the Al_2O_3/Ni composites and the chemical analysis of the elements in selected areas

The XRD pattern of the prepared samples is given in Fig. 4. The pattern corresponds to a sample sintered at 1400 °C. The X-ray diffraction patterns showed no reflections other than those due to alumina and nickel. There was no nickel aluminate spinel phase ($NiAl_2O_4$) in the samples after sintering. The absence of the $NiAl_2O_4$ spinel phase peaks indicates that nickel has not reacted with alumina into nickel aluminate spinel. The reductive atmosphere (H_2/Ar) used during the sintering allowed to avoid the formation of the $NiAl_2O_4$ spinel phase which frequently appears in such processes [21–24].

The results of the measurements of selected physical properties for sintered samples are shown in Table 1. It can be noticed that samples are described by relative density equal to 99.33%. It means that the prepared material is characterized by high degree of packing of the grains in the sintered body. Such high value of relative density was achieved through the use of innovative manufacturing method. The use of centrifugal force allowed to obtain a high density in the green state which facilitated the process of sintering. The linear shrinkage of the sintered samples was 12.84%.

The typical microstructure of the Al_2O_3/Ni composite with different zones of the metal particles concentration is presented in Fig. 5. In the microstructure, the areas with dark contrast represent the Al_2O_3 matrix and with light contrast represent the Ni particles. The results of the observation of the microstructure showed that the obtained samples are characterized by a gradient distribution of the metallic phase throughout the surface of the sample. The changes in microstructure are represented by three zones: from the outer surface toward inner side of the hollow cylinder. It was found that the outer part of the graded region was formed as a result of removing water by the capillary forces active in the gypsum mold. The maximum concentration of the metal particles was observed in the central region of the composites. This part of the sample was formed due to the centrifugal acceleration combined with the capillary action. The metal content decreases continuously from a maximum value to zero in the inner part of samples. The own results of research showed the characteristic sharp transitions between zones in obtained composites [25].

Furthermore, by using the EDS technique, the gradient distribution of Ni particles was confirmed. Figure 6 shows the areas selected to EDS measurements. The research consists in finding the chemical composition in three regions along the gradation direction. The results of the concentration of nickel, alumina and oxygen in composite have been collected in Table 2. Deficit of oxygen in all zones is due to the large error of measurement of light elements like oxygen what is typical for EDS method.

The microstructure of the Al_2O_3/Ni interface is presented in Fig. 7. The observation confirmed that at the phase boundary there are no cracks and other defects. Moreover, there are no new phases at interfaces in the analyzed sample.

Figure 8 shows the histograms of nickel particles size distribution. It was found that histograms have unimodal character for each zone. The analysis of histograms showed in each zone the maximum frequency of metallic particles incidence with an average size 2–3 µm. This value is close to the size of starting nickel powder. It can be concluded that in the obtained composite there are no nickel agglomerates.

The stereological analysis indicated that the metal particles in all zones had the similar oval shape. This is

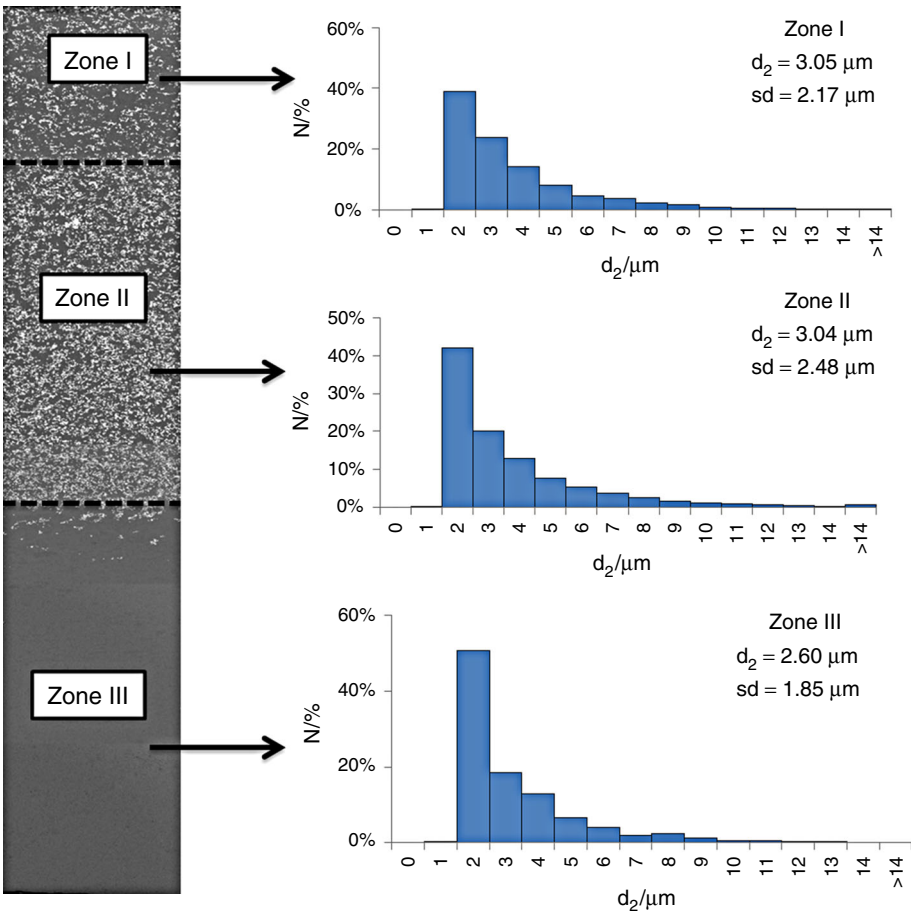

Fig. 8 Distribution of nickel particles in three zones of the Al_2O_3/Ni composites (N—frequency, d_2—diameter, sd—standard deviation)

Table 3 Parameters describing shape factors of metal particles in the Al_2O_3/Ni composite material

Zone	Elongation	Curvature of metal boundary	Convexity
Zone I	1.29 ± 0.09	1.28 ± 0.04	1.06 ± 0.03
Zone II	1.27 ± 0.11	1.31 ± 0.06	1.09 ± 0.02
Zone III	1.14 ± 0.05	1.19 ± 0.04	1.03 ± 0.04

evidenced by the values of shape parameters (the curvature of grain boundary, convexity presented in Table 3). These values are close to one.

Conclusions

Fabrication of Al_2O_3/Ni gradient material by centrifugal-slip casting was done in this study. The microstructure of the outer surface revealed the presence of particles as result of removing water by the capillary forces active in the gypsum mold. The maximum concentration of the metallic particles was observed in the middle part of sample due to the centrifugal acceleration combined with the capillary action. In the inner part of samples, it was observed that the nickel content decreases continuously from a maximum value to zero.

Thermal analysis carried out in the inert atmosphere that is argon and in the reductive atmosphere that is the mixture of hydrogen and argon (1:1) revealed the differences in the total mass loss of the nickel powder what may indicate on the presence of the oxidized formed on the nickel surface. The data obtained from the mass spectrometer coupled with the thermobalance reveal that the predominant gaseous products released from the samples during thermal treatment are H_2O, CO_2 and probably CH_4 in the case of the measurements carried out in H_2/Ar atmosphere.

Acknowledgements The results presented in this paper were obtained within the project from the Polish National Science Centre (NCN), Agreement No. 2013/11/B/ST8/0029.

References

1. Kieback B, Neubrand A, Riedel H. Processing techniques for functionally graded materials. Mater Sci Eng A. 2003;362:81–106. doi:10.1016/S0921-5093(03)00578-1.
2. Suresh S, Mortensen A. Fundamentals of functionally graded materials. Cambridge: Cambridge University Press; 1998. doi:10.1016/S1369-7021(98)80023-0.
3. Miyamoto Y, Kaysser WA, Rabin BH, Kawasaki A, Ford RG, editors. Functionally graded materials, design, processing and applications. Boston: Kluwer Academic Publishers; 1999.
4. Shiota I, Miyamoto Y. Functionally graded materials 1996. Mater Sci Technol. 1996;17B:293–341.
5. Finot M, Suresh S, Bull C, Sampath S. Curvature changes during thermal cycling of a compositionally graded Ni-Al_2O_3 multilayered material. Mater Sci Eng A. 1996;205:59–71. doi:10.1016/0921-5093(95)09892-5.
6. Tuan WH, Brook RJ. Processing of alumina/nickel composites. J Eur Ceram Soc. 1992;10:95–100. doi:10.1016/0955-2219(92)90123-U.
7. Oziębło A, Konopka K, Bobryk E, Szafran M, Kurzydłowski KJ. Al_2O_3-Fe functionally graded materials fabricated under magnetic field. Solid State Phenom. 2005;101–102:143–6. doi:10.4028/www.scientific.net/SSP.101-102.143.
8. Kawasaki A, Watanabe R. Concept and P/M fabrication of functionally gradient materials. Ceram Int. 1997;23:73–83. doi:10.1016/0272-8842(95)00143-3.
9. Zygmuntowicz J, Miazga A, Konopka K, Jedrysiak K, Kaszuwara W. Alumina matrix ceramic-nickel composites formed by centrifugal slip casting. Process Appl Ceram. 2015;9:199–202. doi:10.2298/PAC1504199Z.
10. Zygmuntowicz J, Miazga A, Konopka K, Kaszuwara W. Metal particles size influence on graded structure in composite Al_2O_3-Ni. Mater Technol. 2016;50:537–41. doi:10.17222/mit.2015.120.
11. Gizowska M, Konopka K, Szafran M. Properties of water-based slurries for fabrication of ceramic–metal composites by slip casting method. Arch Metall Mater. 2011;56:1105–10. doi:10.2478/v10172-011-0123-8.
12. Kitakatsu N, Maurice V, Hinnen C, Marcus P. Surface hydroxylation and local structure of NiO thin films formed on Ni(111). Surf Sci. 1998;407:36–58. doi:10.1016/S0039-6028(98)00089-2.
13. Trumble KP, Ruhle M. The Thermodynamics of spinel interface formation at diffusion-bonded Ni/Al_2O_3 interfaces. Acta Metall Mater. 1991;39:1915–24. doi:10.1016/0956-7151(91)90160-3.
14. Schulze D, Schiller WA. Burnout of organic components of glass ceramic composite tapes: thermoanalytical investigations. J Therm Anal Calorim. 1998;52:211–9. doi:10.1023/A:1010186912460.
15. Wiecińska P. Thermal degradation of organic additives used in colloidal shaping of ceramics investigated by the coupled DTA/TG/MS analysis. J Therm Anal Calorim. 2015;123:1419–30. doi:10.1007/s10973-015-5075-1.
16. Gimzewski E. Thermal analysis in reactive atmospheres. J Therm Anal Calorim. 1988;33:159–76. doi:10.1007/BF01914596.
17. Leszczynska A, Pielichowski K. Application of thermal analysis methods for characterization of polymer/montmorillonite nanocomposites. J Therm Anal Calorim. 2008;93:677–87. doi:10.1007/s10973-008-9128-6.
18. Golofit T, Zysk K. Thermal decomposition properties and compatibility of CL-20 with binders HTPB, PBAN, GAP and poly-NIMMO. J Therm Anal Calorim. 2015;119:1931–9. doi:10.1007/s10973-015-4418-2.
19. Hidber PC, Graule TJ, Gauckler LJ. Citric acid—a dispersant for aqueous alumina suspensions. J Am Ceram Soc. 1996;79(7):1857–67. doi:10.1111/j.1151-2916.1996.tb08006.x.
20. Michalski J, Wejrzanowski T, Pielaszek R, Konopka K, Łojkowski W, Kurzydłowski KJ. Application of image analysis for characterization of powders. Mater Sci Pol. 2005;23:79–86.
21. Zygmuntowicz J, Wiecińska P, Miazga A, Konopka K. Characterization of composites containing $NiAl_2O_4$ spinel phase from Al_2O_3/NiO and Al_2O_3/Ni systems. J Therm Anal Calorim. 2016;125:1079–89. doi:10.1007/s10973-016-5357-2.
22. Zygmuntowicz J, Miazga A, Konopka K. Morphology of nickel aluminate spinel ($NiAl_2O_4$) formed in the Al_2O_3–Ni composite system sintered in air. Compos Theory Pract. 2014;14:106–10.
23. Tuan WH, Lin MC. Reaction sintering of Al_2O_3/$NiAl_2O_4$ composites. J Mater Sci Lett. 1996;15:735–7.
24. Tuan WH, Wu HH, Chen RZ. Effect of sintering atmosphere on the mechanical properties of Ni/Al_2O_3 composites. J Eur Ceram Soc. 1997;17:735–41.
25. Zygmuntowicz J, Miazga A, Konopka K, Kaszuwara W. Structural and mechanical properties of graded composites Al_2O_3/Ni obtained from slurry of different solid content. Struct Integr Proced. 2016;1:305–12. doi:10.1016/j.prostr.2016.02.041.